Journal of Environmental Management 176 (2016) 34–44

Contents lists available at ScienceDirect

Journal of Environmental Management

journal homepage: www.elsevier.com/locate/jenvman

Research article

Electrocoagulation using a rotated anode: A novel reactor design for textile wastewater treatment

Ahmed Samir Naje [a], Shreeshivadasan Chelliapan [a, c, *], Zuriati Zakaria [b], Saad A. Abbas [a]

[a] Department of Engineering, UTM Razak School of Engineering and Advanced Technology, Universiti Teknologi Malaysia, Jalan Semarak, 54100, Kuala Lumpur, Malaysia

[b] Department of Environmental Engineering and Green Technology, Malaysia-Japan International Institute of Technology (MJIIT), Universiti Teknologi Malaysia, Jalan Semarak, 54100, Kuala Lumpur, Malaysia

[c] Centre for Environmental Sustainability and Water Security (IPASA), Research Institute for Sustainable Environment, Block C07, Level 2, Universiti Teknologi Malaysia, 81310, Johor Bahru, Johor, Malaysia

ARTICLE INFO

Article history:
Received 18 February 2015
Received in revised form
25 June 2015
Accepted 22 March 2016

Keywords:
Electrocoagulation
Electrode consumption
Textile wastewater
Rotated anode reactor

ABSTRACT

This paper investigates the optimum operational conditions of a novel rotated bed electrocoagulation (EC) reactor for the treatment of textile wastewater. The effect of various operational parameters such as rotational speed, current density (CD), operational time (RT), pH, temperature, and inter-electrode distance (IED) on the pollutant removal efficiency were examined. In addition, the consumption of aluminum (Al) and electrical energy, as well as operating costs at optimum conditions were also calculated. The results indicated that the optimum conditions for the treatment of textile wastewater were achieved at CD = 4 mA/cm^2, RT = 10 min, rotational speed = 150 rpm, pH = 4.57, temperature = 25 °C, and IED = 1 cm. The electrode consumption, energy consumption, and operating costs were 0.038 kg/m^3, 4.66 kWh/m^3 and 0.44 US$/m^3, respectively. The removal efficiencies of chemical oxygen demand (COD), biological oxygen demand (BOD), total suspended solid (TSS), turbidity and color were 97.10%, 95.55%, 98%, 96% and 98.50%, respectively, at the first 10 min of reaction time, while the phenol compound of the wastewater was almost entirely removed (99.99%). The experimental results confirm that the new reactor design with rotated anode impellers and cathode rings provided high treatment efficiency at a reduced reaction time and with lower energy consumption.

1. Introduction

The electrocoagulation (EC) process comprises the in-situ generation of coagulants with the dissolution of the sacrificial anode. The anode is commonly made of aluminum or iron (Chen, 2004). The metal ions react with the cathode generating OH^- ions. This reaction produces insoluble hydroxides that adsorb the pollutants and eliminate them from the solution either by complexation or by electrostatic attraction, that followed by coagulation (Dalvand et al., 2011). Among the most critical tasks in decreasing the overall cost of EC operation is the reduction of the internal resistance drop of the electrodes (IR-drop) to improve the performance of the current. This issue may be mitigated by improving the state of turbulence, and at the same time, the mass transport may be improved by increasing the turbulence state within the flow via an EC reactor. Alternatively, the turbulence may be raised by raising the flow rate rather than the EC reactor. The increase in the turbulence state also decreases the passivation at the electrode plates. Both hydrogen and oxygen gas are evolved near the anode and cathode as each gas bubble nucleates. These bubbles are in the form of insulating spherical figures, and if permitted to gather on the surfaces of the electrode, would increase the cell's overall electrical resistance, thus requiring a greater amount of electrical energy to obtain the optimum removal efficiency. To mitigate the accumulation of bubbles, the flow of the electrolyte surrounding the electrodes must be increased to push the bubbles out (Mollah et al., 2004).

From a mechanical point of view, stirred tanks are utilized for a great variety of industrial software applications, such as the utilization of chemical reactions within liquids, the fusion of miscible based liquids, the liquid-liquid distribution of immiscible liquids, and the suspension of solids, among other applications. Multiple

* Corresponding author. Department of Engineering, UTM Razak School of Engineering and Advanced Technology, Universiti Teknologi Malaysia, Jalan Semarak, 54100, Kuala Lumpur, Malaysia.
E-mail address: shreeshivadasan.kl@utm.my (S. Chelliapan).

http://dx.doi.org/10.1016/j.jenvman.2016.03.034
0301-4797/

parameters that illustrate hydrodynamic operations are conventionally utilized to analyze the general mixing process within stirred tanks. Some of these parameters are the flow velocity field output from an impeller and the intensity of the turbulence acting as the main function of the rate of agitation and the overall distance to the impeller. These parameters are often utilized practically, including scenarios in which the general local turbulence ceases to be isotropic (Oldshue, 1983). Generally, the dispersion of the turbulence intensity value within the vessel is an estimate of the micro-mixing operations, where the momentum blending, as a result of fluctuations in turbulent velocity (applied on the main motion), supplies the final blending (Paul et al., 2004).

The overall intensity of the turbulence is the main reason for the micro-mixing operations (eddy diffusion of the momentum), heat values and mass values (Rahim et al., 2011). Consequently, micro-mixing operations limit the overall development of rapid reactions. Based on the previous discussions, the overall efficiency of the stirred tank reactor is clearly found to primarily rely on the general properties of both the turbulent intensity and the pattern flow produced by the impeller. As a result, multiple studies have focused on the identification of the hydro-dynamical properties of the main flow created by standard impeller types and their association with the most significant design parameters, such as the off-bottom distance of the impeller, the diameter of the impeller in relation to the diameter of the tank, the depth of liquid, the impeller spacing, the vessel's aspect ratio, the bottom of the tank, and the shape and size of the baffles (Kresta and Wood, 1993; Nienow, 1997; Mishra et al., 1998; Jaworski et al., 2001; Roya et al., 2010; Singh et al., 2011).

The EC approach is a clean technology. However, in the operation, an oxide-based fouling film is created over the surface of the electrode (passivation effects) within electrochemical-based reactors that do not contain static electrodes or liquid mixing due to the poor diffusion and transfer of mass. This poor diffusion and mass transfer decrease the operation's overall performance levels and increase the overall consumption of energy (Martínez-Delgadillo et al., 2000).

To address these effects, in this study, the overall efficiency of an EC reactor that includes rotating aluminum (Al) electrodes of various electrode speeds was analyzed and practical investigations were conducted to formulate the main design and operation parameters required to improve the overall efficiency of these types of reactors (Martínez-Delgadillo et al., 2012). In addition, the main goal of this study is to investigate the textile wastewater treatment in terms of the requirements of legal discharge, with no further treatment, by using a custom-tailored EC reactor under the best operational conditions.

2. Materials and methods

2.1. Wastewater characteristics

The wastewater used in this work was collected from a major textile-based industry in Iraq (Babylon). The industry uses the Imperon Violet KB (CAS #: 6358-46-9) for the fabric dyeing process. Tables 1 and 2 present the main characteristics of the textile wastewater and the properties of the Imperon Violet KB, respectively.

2.2. EC rotating anode reactor

The novel EC reactor that is used in this investigation is illustrated in Fig. 1. The reactor (10 L) had a stirred tank setting of a cylindrical form (external diameter, 180 mm; inner diameter, 174 mm; total length, 500 mm) and was constructed from Perspex.

Table 1
Characteristics of textile wastewater.

Parameters	Values
Electrical conductivity (μS/cm)	1455
Turbidity (NTU)	396
Total suspension solid, TSS (mg/L)	3270
Total dissolved solid, TDS (mg/L)	1250
Dissolved oxygen, DO (mg/L)	0.72
pH	4.50
Chlorides, Cl^- (mg/L)	35
Sulfate (mg/L)	678
Phosphate (mg/L)	7.2
Nitrates (mg/L)	11
Phenols (mg/L)	335
Oil & grease (mg/L)	3.2
BOD (mg/L)	112
COD (mg/L)	990

Table 2
Properties of Imperon Violet KB.

Color	Imperon Violet KB
Chemical structure	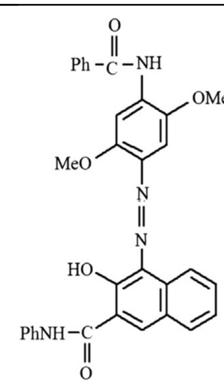
Chemical formula	$C_{32}H_{26}N_4O_5$
Molecular weight (g/Mol)	546.57
λ max (nm)[a]	533

[a] Absorbance of 0.34 at 533.

A rotating shaft (diameter, 32 mm) was attached to an adjustable speed motor in order to hold the impeller structure and also to maintain the electrode rotations. The motor is AC electrical type and supplies various steady state speeds (0–1000 rpm, 0–5A, 220 V, USA). The electrodes were composed of aluminum (Al) substance. The rotating anode consists of 10 impellers. Each impeller consists of four main rods (length, 30 mm; diameter, 12 mm), with 10 rings used as a cathode. Each ring (diameter, 172 mm; internal diameter, 134 mm; thickness, 12 mm) was arranged sequentially at a distance of 30 mm apart from each other. The total active surface area was 500 cm^2, and contains three equally spaced baffles in order to stop the rotation and mass fluid's tangential flow arrangements and also to establish the cathode rings.

2.3. Experimental procedure

EC reactor performance was characterised in terms of COD, TSS and color removal. The experiment was carried initially by studying the effect of rotational speed of anode and current density. The overall efficiency of the reactor was tested using three main variables; processing time, current density and the anode's overall rotational speed. The electrolysis time (RT) was maintained in the range of 10–30 min. Three main current densities (CD); 4, 6 and 8 mA/cm^2 with various steady state anode rotational speeds of 75,

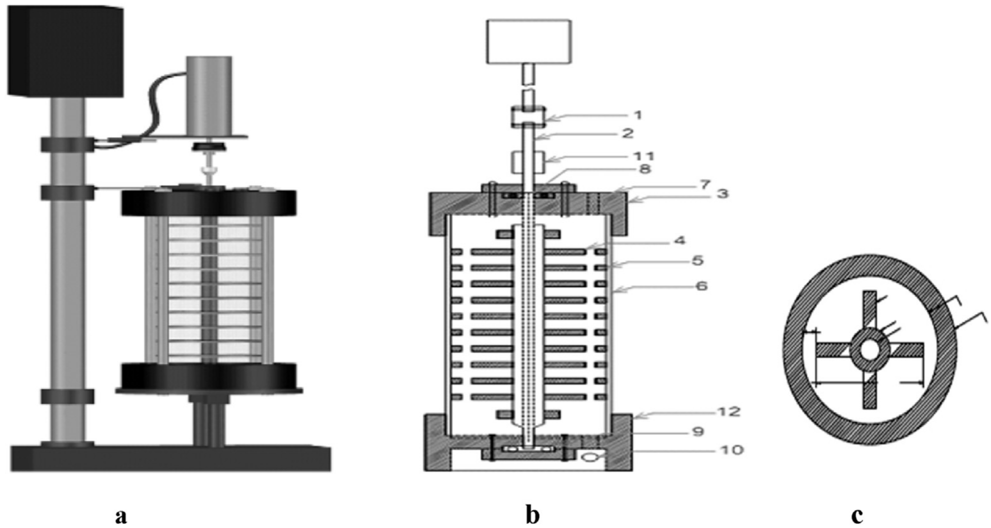

Fig. 1. a. Schematic diagram of EC rotated anode system. b. Details of EC rotated anode reactor: 1. Motor varible speed; 2. Stainless steel shaft (D = 32 mm); 3. Upper teflon flange cover (D = 280 mm, H = 100 mm); 4. Al rods of impellers anode (no = 4, L = 30 mm, D = 12 mm); 5. Al rings of cathode (no = 10, D.out = 172 mm, D.in = 132 mm, T = 12 mm); 6. Perspex reactor (D.out = 180 mm, D.in = 174 cm, L = 500 mm); 7. Upper ports (no = 3, D = 10 mm); 8. Ball bearing; 9. Thrust bearing; 10. Lower port (D = 10 mm); 11. Zoom couping; 12. Lower teflon flange cover (D = 280 mm, H = 100 mm). c. Top view of impellers anode with ring cathode.

150 and 250 rpm were examined at an ambient temperatures (25–27 °C). The three current densities were chosen based on some initial investigations and the results showed that there was no significant effect to the overall removal efficiency when the current densities were increased above 8 mA/cm^2. In every execution, a 10 L sample was utilized for the operation of EC treatment, and EC batch rounds were executed at nine different times. A primary sample was extracted and subsequently. At the end of each round, the cells were cleaned with a 5% hydrochloric acid solution for a period of 10 min and later scrubbed with a sponge. Both the cathode and anode were attached to the negative and positive parts of DC power supply (YIZHAN, 0–40 V; 0–6 A, China). The main voltage was 30 V for each run. A voltmeter was connected in parallel with the cell to measure its voltage. The current was maintained as invariant in every round with the use of a variable resistance and estimated with use of an ammeter (Aswar DT830D, China). In every iteration, the samples were allowed to settle for 30 min and then filtered. Approximately 100 ml of supernatant sample was gathered for analysis and investigation in replicate. Similar parameters were estimated in every replicate sample.

The experiment was carried out at four different operational parameters to obtain greater optimal conditions. The effect of pH on the EC process was carried out at different pH values. The pH was gradually increased from 5 to 10 by adding 0.5 M NaOH during the experiment. A particular number of supporting electrolytes such as NaCl and Na_2SO_4 (0.0, 0.02, 0.05, and 0.10 kg/m^3) were introduced into the wastewater to investigate the impact electrolysis support on the removal performance. The effect of temperature was carried out in the range of 25–45 °C using water circulation (WiseCircu Model WCR-P6) to maintain the temperature during EC process. Inter electrode distance between the impellers of the anode and rings of the cathode were achieved for distances between 1, 1.5 and 2 cm. Towards the completion of the experiment, the optimum operational condition was carried out again in triplicate to validate the EC process's accuracy and reproducibility for treating the textile wastewater contaminants.

2.4. Chemical analysis

The overall treatment performance of the novel electrolysis was analyzed in terms of COD, TSS and color removal performances. The electrical potential was maintained at 30 V for each iteration. The COD was estimated by a Closed Reflex-Titrimetric method. The TSS and TDS were measured by Gravimetric method. Phenol was examined by high-performance liquid chromatography (HPLC), Agilent Technology 1200 series. ODS hypersil C18 column (4.6 mm × 150 mm × 5 μm) at 25 was used as the separation column for phenol and aromatic compounds using acetonitrile/water (60/40, v/v) as the mobile phase. The injection volumes and the mobile phase flow rate were 5 μL and 1 ml/min respectively. The detection wavelength was set at 254 nm. The samples were filtered through a 0.25 μm membrane filter. The oil and grease (O&G) was estimated by Solvent Extraction method. The BOD and DO (dissolved oxygen) were measured by DO meter (Eutech Instrument Cyberscan 110). The pH (model pHM84), conductivity (HANNA HI-99301), and turbidity (HACH 2100P) were also investigated in this study. The color was determined via absorbance with a UV–Vis Spectrophotometer (Shimadzu UV 1700) with a wavelength that corresponds to the peak absorbance value for textile wastewater (533 nm). The samples were filtered using Whatman 934 AH filter. The rotational speed of the rotated anode was maintained by a microprocessor digital meter. Ion analysis was performed using ionic chromatography ICS-2000. All the analytical work was conducted according to the procedures prescribed in the standard methods (APHA, 2000). The computation of TSS, COD and color removal was carried out using formulas specified by among others (Un and Aytac, 2013; Bayar et al., 2011; Merzouk et al., 2010; Aoudj et al., 2010).

2.5. Economic analysis

The operation cost in the wastewater treatment consists of the electricity costs, sludge disposal cost, the chemical reagents, maintenance, labors, and equipment. During the electrochemical operation, the most significant parameters that impact the operating cost are the cost of the consumed electrical energy and the electrode material. Therefore, these factors are computed in this investigation to identify the overall operating costs (Dalvand et al., 2011):

a)

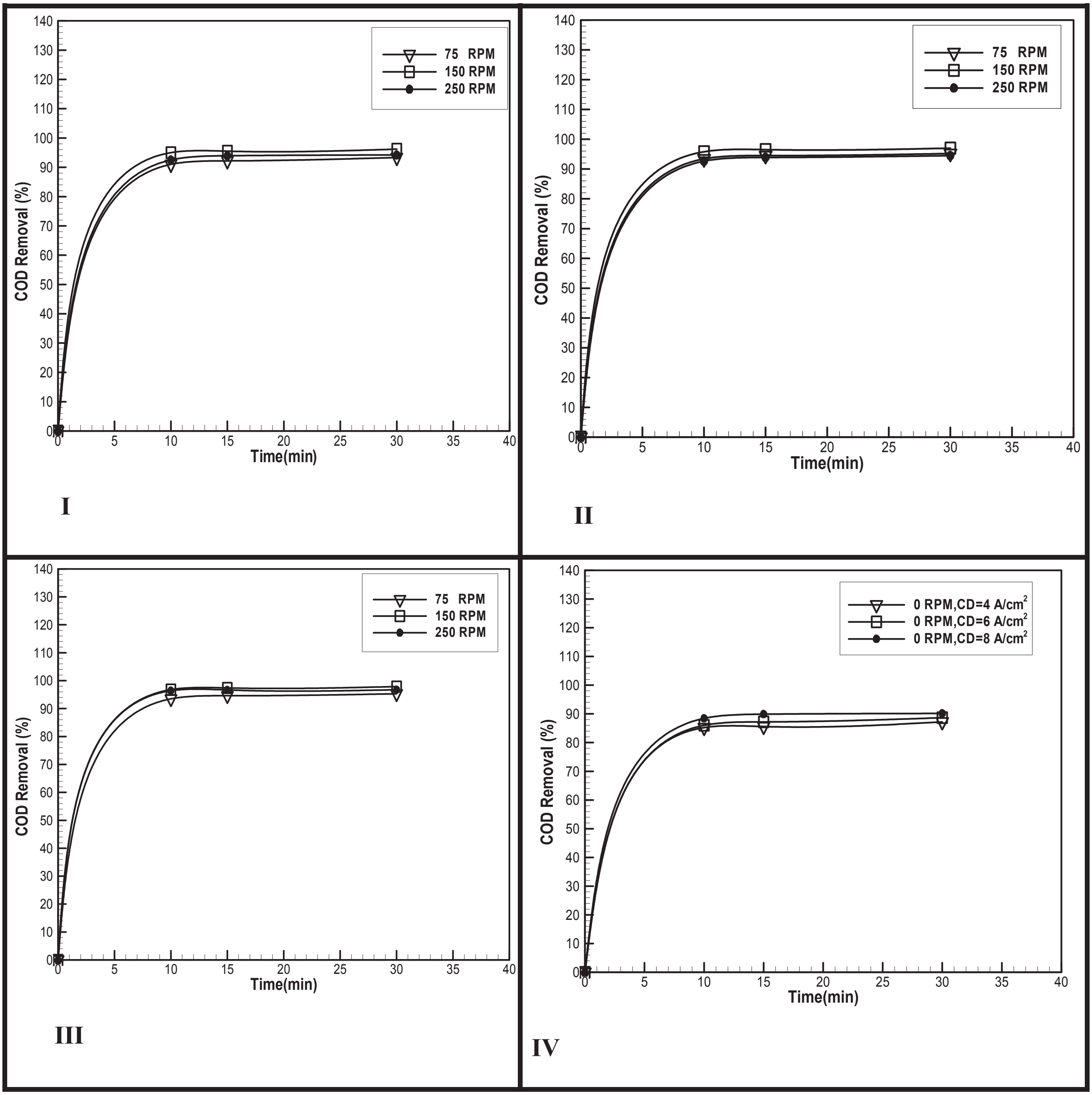

Fig. 2. a. Effect of rotational speed on COD removal, I. CD = 4 mA/cm^2; II. CD = 6 mA/cm^2; III. CD = 8 mA/cm^2; IV. Zero rotational speed. b. Effect of rotational speed on TSS removal, I. CD = 4 mA/cm^2; II. CD = 6 mA/cm^2; III. CD = 8 mA/cm^2; IV. Zero rotational speed. c. Effect of rotational speed on color removal, I. CD = 4 mA/cm^2; II. CD = 6 mA/cm^2; III. CD = 8 mA/cm^2; IV. Zero rotational speed.

$$\text{Operating cost} = a\, C_{energy} + b\, C_{electrode} \quad (1)$$

$$C_{energy} = U \cdot I \cdot t / V \quad (2)$$

where C_{energy}, $C_{electrode}$, a, b, U, I, t and V represent energy consumption for each cubic meter of wastewater (kWh/m^3), electrode consumed for treatment of one cubic meter of wastewater (kg/m^3), electricity cost 0.075US$/kWh and standard cost of aluminum 2.5 US$/kg, voltage (V), current (A), residence time (h) and volume of wastewater (L), respectively.

In this study, the overall electrical energy consumption was computed based on the following equation:

$$C_{energy}\ (\text{kWh/m}^3) = (C_{energy})_S + (C_{energy})_M \quad (3)$$

where $(C_{energy})_S$ represents the value of the electrical energy

b)

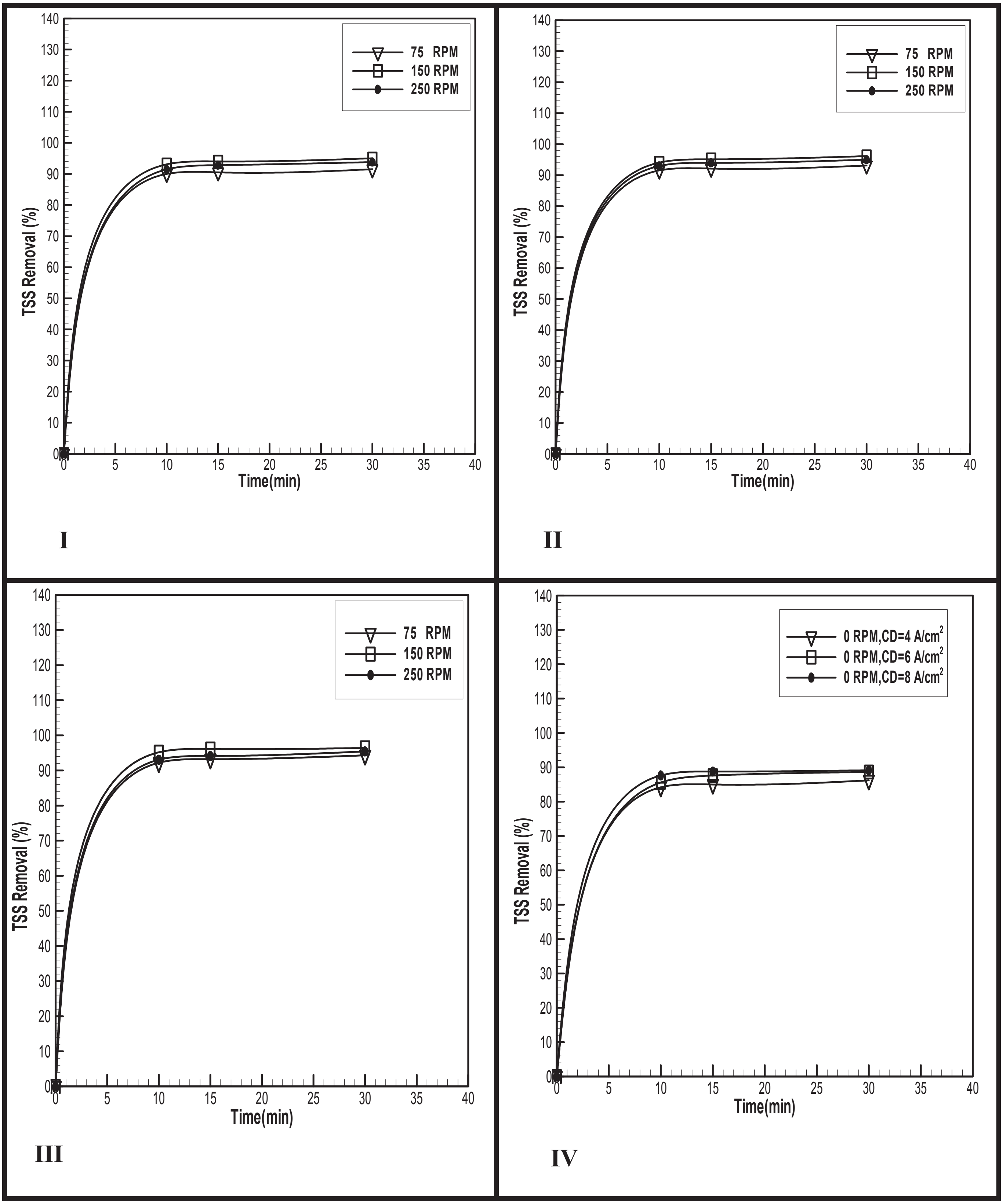

Fig. 2. (*continued*)

c)

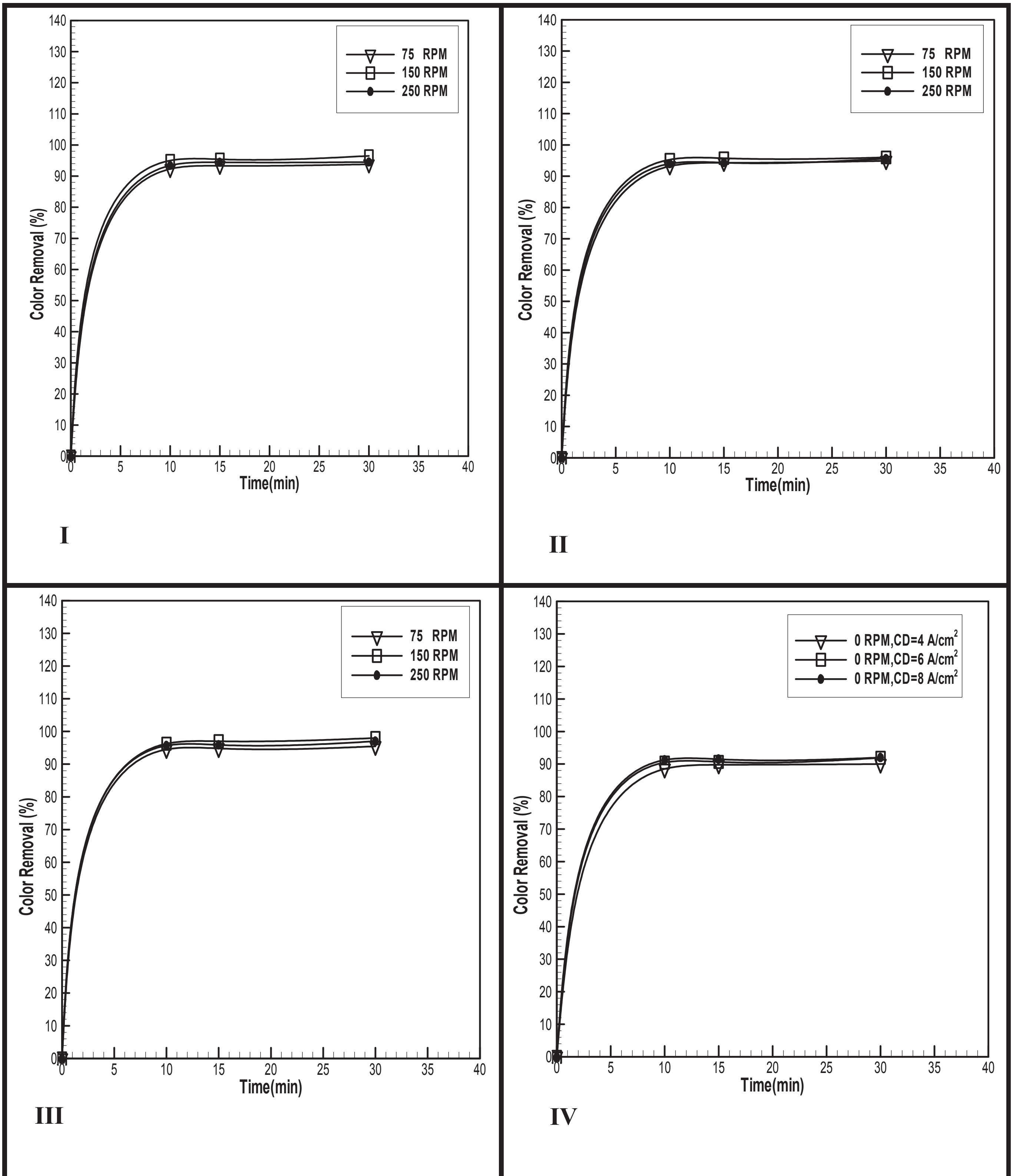

Fig. 2. (*continued*)

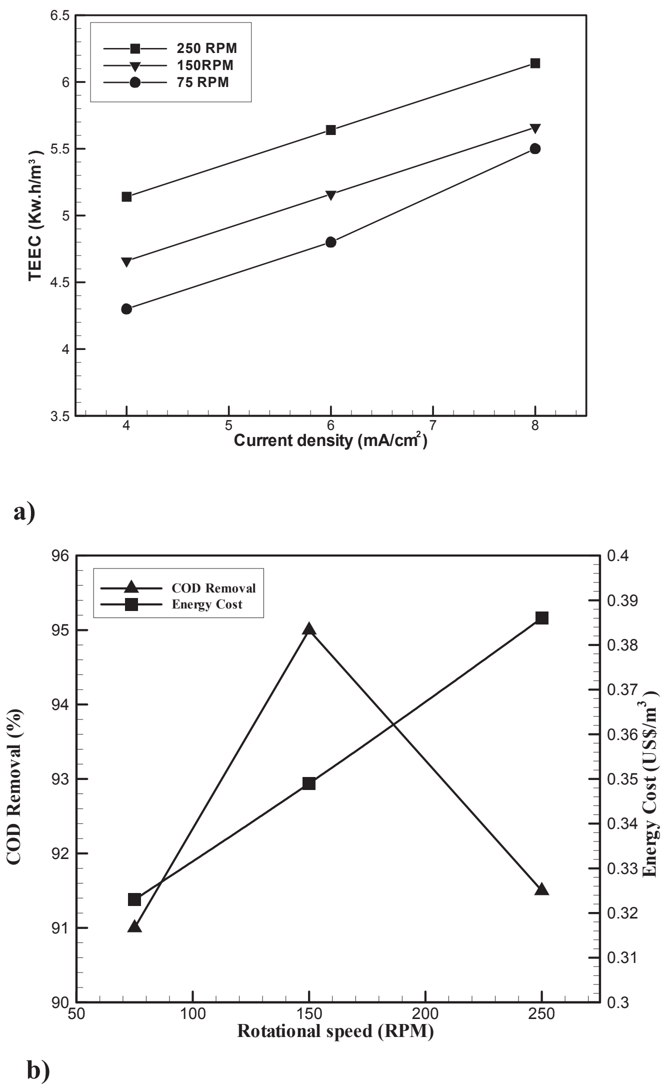

Fig. 3. a) Effect of current density and rotational speed on electrical energy consumption at reaction time = 10 min; b) Effect of rotational speed on COD removal and energy cost at CD = 4 mA/cm^2 and reaction time = 10 min.

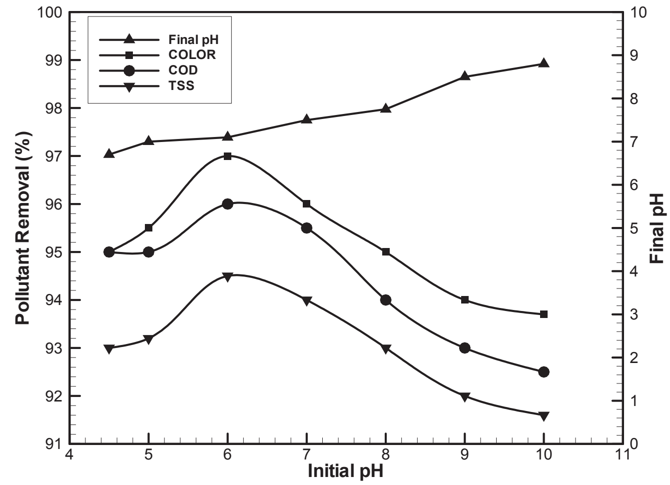

Fig. 4. Influence of initial pH on COD removal under optimal conditions (CD = 4 mA/cm^2, RT = 10 min, rotational speed = 150 rpm).

consumption of the reactor (electricity input to the anode and the cathode due to DC power supply), and $(C_{energy})_M$ represents electrical energy consumption rate of the AC motor anode rotation. Both the $(C_{energy})_S$ and $(C_{energy})_M$ was computed from Eq. (2). The operating expense is computed based on the prices acquired from the Iraqi market in the year 2014.

3. Results and discussion

3.1. Effect of rotational speed of anode and current density

The primary operation of the rotational speed is to efficiently move the coagulant substance that is formulated by the electrodes dissolution to the reactor. Under the condition that the coagulant substance does not become distributed within the reactor in an efficient manner, the reactor's contents are not homogenous, and consequently, regional variations may be observed. The rotational speed may also lead to the homogenization of the reactor variables, including the temperature and pH (Bayar et al., 2011). On the other hand, high rotational speed can potentially damage flocs that are formed within the reactor, and create smaller flocs that are not easy to extract from the water. In this study, the impact of rotational speed was analyzed at 0, 75, 150 and 250 rpm, with current densities (CD) of 4, 6 and 8 mA/cm^2 and with the electrolysis time (RT) of 10–30 min. In terms of a stirred tank, the Reynolds number is commonly utilized (Martínez-Delgadillo et al., 2013):

$$Re = \rho \, N \, D^2/\mu \quad (4)$$

where ρ = density, μ = viscosity, D = impeller bar length (at D = 9 cm), and N = impeller revolutions (per second). At standard room temperature (25 °C), the wastewater viscosity and density are $\mu = 0.8937 \times 10^{-3}$ Pas and $\rho = 997.04$ kg^{-3} respectively. When the rotational speed (N) is 75, 150, and 250 rpm, the corresponding Reynolds number (*Re*) was 1.13×10^4, 2.26×10^4 and 3.76×10^4 respectively. This confirms that it is an entirely turbulent flow ($Re > 10^4$). Based on the experimental results depicted in Fig. 2a (i to iv), if the anode was static with no rotational speed (CD = 8 mA/cm^2), the corresponding COD removal efficiency was 90%, in a time period of 30 min. The COD removal efficiency increased to 91% within 10 min (processing time reduced by 20 min) when the reactor was operated at a rotational speed of 75 rpm and reduced current density (CD = 4 mA/cm^2). Further increases in rotational speed (150 rpm), resulted in higher COD removal (95%), at the same operating conditions of reaction time (10 min) and current density (4 mA/cm^2). During this period, the formulated Al $(OH)_3$ flocs was connected to each other and the precipitation was easier. However,

Table 3
Current efficiency at optimum condition (RT = 10 min, rotational speed = 150 rpm).

Current density mA/cm^2	Al^{+3}_{exp} (mg/L)	$Al^{+3}_{theoretical}$ (mg/L)	Current efficiency (%)
4	38.00	11.18	339
6	58.00	16.77	346
8	78.00	22.36	349

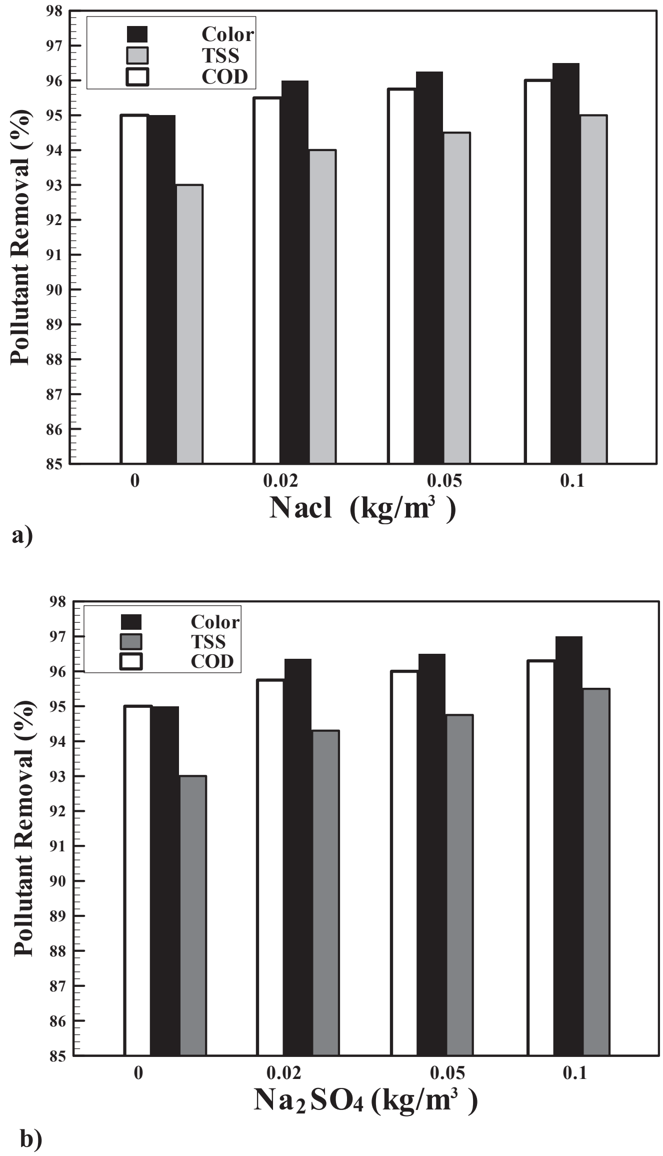

Fig. 5. Effect of electrolysis support on COD, TSS and color removal under optimal conditions (CD = 4 mA/cm^2, RT = 10 min, rotational speed = 150 rpm, and pH = 4. 55) at different concentrations, a) NaCl and b) Na_2SO_4.

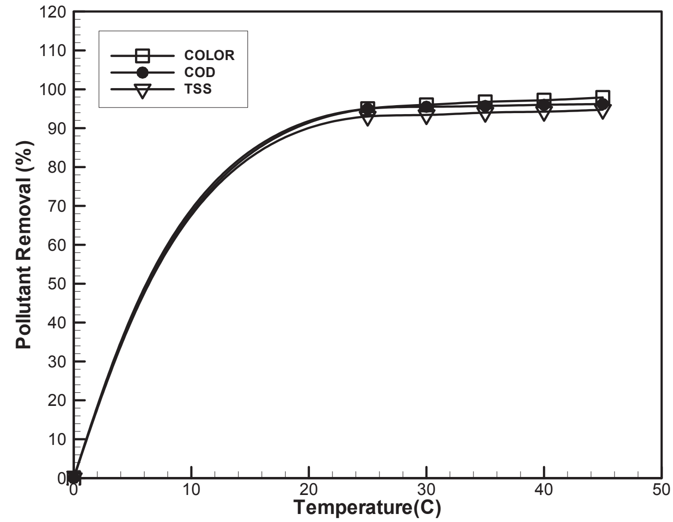

Fig. 6. Effect of temperature on the removal efficiencies of COD, TSS and color (CD = 4 mA/cm^2, RT = 10 min, rotational speed = 150 rpm, pH = 4.55).

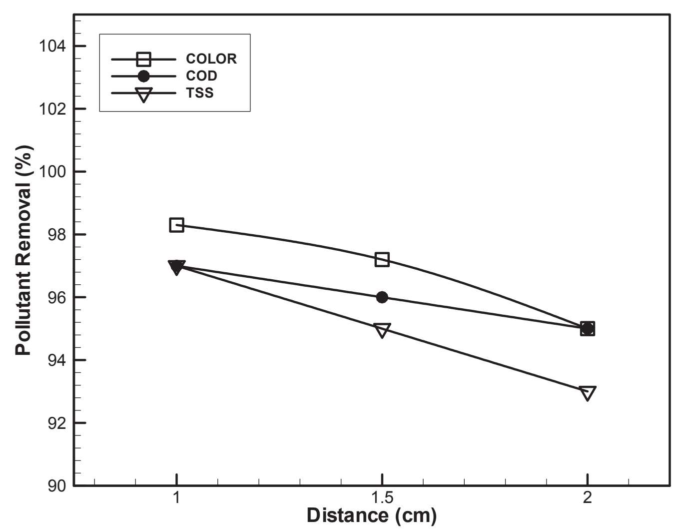

Fig. 7. Effect of inter electrode distance on removal efficiency of COD, TSS and color (CD = 4 mA/cm^2, RT = 10 min, rotational speed = 150 rpm, pH = 4. 55 and T = 25 °C).

when the rotational speed was increased to 250 rpm, no COD removal efficiency was observed probably due to the extremely high rotational speed (Bayar et al., 2011). It should be mentioned here that the increase in the overall current density leads to an increase in the COD removal efficiency (Aoudj et al., 2010). As depicted in Fig. 2a (i − iii), more than 95% COD removal efficiency was observed for all the applied current densities (at 150 rpm and 10 min of reaction time).

The main results were in line with the remaining contaminated properties of TSS and color at all the current density (Fig. 2b (i − iii) and c (i − iii)), and also for all rotational (Fig. 2b (iv) and c (iv)). The color was decreased from 0.34 to 0.0171, 0.0135, and 0.0085 during the initial 10 min with a rotational speed of 150 at current density of 4, 6 and 8 mA/cm^2 respectively. The overall electrical energy consumption due to current densities and motor rotational speed is computed where the current motor of rotating anode were 0.9, 1 and 1.13 A for 75, 150 and 250 rpm respectively with voltage of 220 V.

Fig. 3a depicts the transformation of consumption of electrical energy with the current density at different conditions (75, 150, 250 rpm, 10 min). The electrical energy consumptions were increased when the current densities and the rotational speed of anode were increased. The energy consumption was less (4.66 kWh/m^3) at 150 rpm and CD = 4 mA/cm^2 compared at 75 rpm and CD = 6 mA/cm^2 (4.80 kWh/m^3) and more than at 75 rpm and CD = 4 mA/cm^2 (4.30 kWh/m^3). The difference in energy consumption of EC process at current density of 4 mA/cm^2 when the rotational speed increased from 75 to 150 rpm was 0.3 kWh/m^3 and considered no significance as compared with the increasing in process efficiency at 150 rpm. Fig. 3b illustrates the energy cost with COD removal efficiency at current density 4 mA/cm^2, the reaction time of 10 min for all rotational speed. The result showed that the best performance of EC process at 150 rpm and a minor difference in energy cost (0.02US$/m^3) between 75 and 150 rpm. The energy cost increases when the rotational speed increase to 250 rpm (0.386US$/m^3). The current performance is a critical parameter that impacts the overall electrode lifetime in

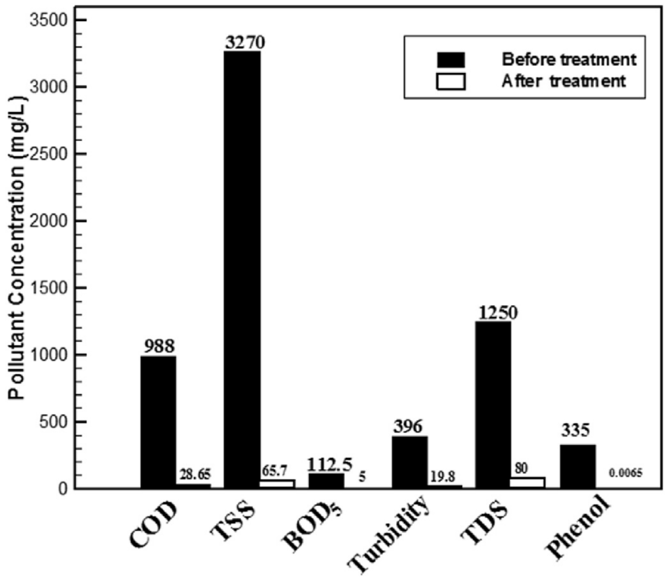

Fig. 8. The removal efficiency of various variables of the textile wastewater under optimal condition (CD = 4 mA/cm^2, RT = 10 min, rotational speed = 150 rpm, pH = 4. 57, Temperature = 25 °C, IED = 1).

electrocoagulation operation. Abdel-Gawad et al. (2012) reported that the efficiency of the current is the ratio of the used amount of Al (ΔM_{exp}) to the overall theoretical value (ΔM_{theo}):

$$C.E = \Delta M_{exp}/\Delta M_{theo} * 100 \quad (5)$$

The level of theoretical Al dissolution is computed based on Faraday's law (Abdel-Gawad et al., 2012):

$$Al^{+3}{}_{theoretical} = M\ I\ RT/ZF\ V \quad (6)$$

where M = molecular mass of Al (26.98 g/Mol), I = electrical current (A), RT = reaction time of EC (sec), Z = amount of electron moles (3), F = Faraday's constant (96,500 c/Mol), and V = volume of wastewater (L). The Al amount used was determined by a weighting process on the electrodes prior and subsequent to every iteration, and the weight loss for the Al was computed. The final results are presented in Table 3, where the ratio of the actual consumption over the theoretical values increased with the increasing current densities. Based on these general regulations, EC treatment under 4 mA/cm^2, 150 rpm and 10 min reaction time is typically required.

3.2. Effect of initial pH

Because pH is a critical operational parameter, numerous research works have been performed that focus on the impact of pH on the electrocoagulation of various types of wastewater (Aoudj et al., 2010; Koparal et al., 2008; Bensadok et al., 2008). In this study, the impact of pH (5–10) on the removal of COD, TSS and color of the textile wastewater was performed under optimal conditions (4 mA/cm^2, 150 rpm and 10 min of reaction time). The initial pH impacts the overall stability of the produced hydroxide species, which affects the performance of the removal process (Aoudj et al., 2010). The best performance of the EC reactor was observed at pH 6 (Fig. 4), with removal efficiencies of COD, TSS, and color of 96%, 94.5%, and 97%, respectively. A minor increase in the final pH was noted in the acidic solution (pH = 4.55, 5 and 6) because the pH levels were estimated in liquid-based fractions (subsequent to the sedimentation of the metallic sludge). This result is probably due to the increase in the hydroxide ion (OH^-) concentration that is created in the solution from the water reduction near the cathode (Canizares et al., 2009). A minor decrease in the overall pH levels in alkaline solution (pH = 10) was noted (pH = 8.8) when compared with the acidic solution, where the ionic structure of Al $(OH)_4^-$ is formed as given by Eq. (7) (Chen, 2004):

$$Al\ (OH)_3 + OH^- \rightarrow Al\ (OH)_4 \quad -(7)$$

With the pH levels of the textile wastewater (pH = 4.55), the removal performances of COD, TSS, and color were 95%, 93%, and 95%, respectively. This result shows that the pH levels of the

Table 4
Effectiveness and reproducibility of the performance of EC rotated anode in treating textile wastewater at optimal conditions (CD = 4 mA/cm^2, RT = 10 min, rotational speed = 150 rpm, pH = 4. 57, Temperature = 25 °C, IED = 1 cm).

Parameters	Raw effluent	Treated effluent	Allowable Limit (EPA) 1996[a]	Removal (%)
Electrical conductivity (μS/cm)	1455	2000	ID	–
Initial pH	4.57	4.57	–	–
Final pH	–	6.92	6–8	–
Energy consumption (kwh/m^3)	–	4.66	–	–
Electrode consumption (kg/m^3)	–	0.038		–
O&G (mg/L)	3	0.1	5–40	96.66
BOD_5 (mg/L)	112.5	5.00	5–45.5	95.55
COD (mg/L)	988	28.65	20–500	97.10
TSS (mg/L)	3270	65.70	60–300	98.00
Color observance at 533 NM	0.3400	0.0051	ID	98.50
TDS (mg/L)	1250	80.00	5–180	93.60
Turbidity (NTU)	396	19.80	15–50	96.00
DO (mg/L)	0.7	14.5	4.5–15	
Sulfate (mg/L)	678	17.00	ID	97.50
Phosphate (mg/L)	7.2	0.23	ID	96.80
Nitrates (mg/L)	11	0.2	ID	98.18
Phenols (mg/L)	335	0.0065	10	99.99
Chlorides Cl^- (mg/L)	33	0.4	ID	–
Aluminum (mg/L)	1.50	6.00	–	__
Electrical energy cost (US$/m^3)	__	0.349	–	__
Electrode consumption cost (US$/m^3)	__	0.095	–	__
Total operating cost (US$/m^3)	__	0.444	–	__

ID: Insufficient Data.
[a] EPA/625/R-96/004 Sep-1996, VOL-1, Appendices.

wastewater with modifications did not exhibit a great impact on the removal efficiencies, and the current results are compatible with the studies of Un and Aytac (2013). Consequently, more experiments and investigations were performed on the standard pH levels of the wastewater to prevent the waste of chemicals in terms of environmental and economic considerations.

3.3. Effect of electrolyte support

The introduction of an electrolyte such as NaCl or Na_2SO_4 into the solution may enhance the conductivity of the wastewater, reduce the cell voltage at constant current density and minimize the amount of consumed electrical energy (Daneshvar et al., 2006; Merzouk et al., 2010). In this study, NaCl and Na_2SO_4 (0.0, 0.02, 0.05, and 0.10 kg/m^3) were introduced into the textile wastewater for the evaluation of the impact of the conductivity on the removal of COD, TSS, and color (Fig. 5a and b). With optimal conditions, the introduction of NaCl and Na_2SO_4 does not greatly modify the removal of COD, TSS and color, as highlighted by Chen et al. (2000). With the introduction of NaCl and Na_2SO_4, the COD removal efficiencies were 95.5%, 95.7%, and 96% for NaCl at 0.02, 0.05 and 0.10 kg/m^3, respectively, and 95.73%, 96% and 96.3% for Na_2SO_4 at 0.02, 0.05 and 0.10 kg/m^3, respectively. The difference in energy consumption due to lower voltage was 0.033 kWh/m^3 and 0.05 kWh/m^3 with the addition of NaCl and Na_2SO_4, respectively. This difference in the energy consumption that was observed between the analysis in the absence and presence of a supporting electrolyte was considered to be unimportant. This result may be compared with the investigation performed by Drogui et al. (2008) by identifying relations that are similar. Additionally, the actual costs increase with the introduction of these particular chemicals.

3.4. Effect of temperature

The overall temperatures were modified to the levels mentioned in the investigation prior to treatment and remained constant in the EC treatment, sedimentation and filtration processes. Fig. 6 depicts the removal efficiency of COD, TSS, and color under the optimal conditions. Note that the general removal values of COD, TSS and color were increased when there was an increase in the temperature (95%–96.2% for COD, 93%–94.75% for TSS, and 95%–97% for the color). The temperature impacts the rate of contaminant removal through the following factors (Laidler and Meister, 1999): (i) an increase in the temperature creates an increase in the rate of Al^{3+} hydrolysis to $Al(OH)_3$, and (ii) an increase in the temperature creates an increase in the diffusivity of Al^{3+} based on the Stokes-Einstein's standard equation; as a result, an increase was observed in the mass transfer rate of Al^{3+} from the surface of the anode to the solution bulk. With a temperature greater than 40 °C, the Al $(OH)_3$ solubility within the solution increases with a resulting loss of the coagulant (El-Ashtoukhy et al., 2013). With the current conditions, the improvement effects are found to be greater than the adverse effects.

3.5. Effect of the inter distance between impellers anode and rings of cathode

Numerous researchers have investigated the impact of the overall electrode distance on the efficiency of pollutant removal. According to these works, the main evolution of the EC efficiency levels as a standard function of inter-electrode distance is found to rely on the nature of the pollutant, the structure of the electrodes, and the hydrodynamic conditions, among others (Modirshahla et al., 2007, 2008; Daneshvar et al., 2004). In the current investigation, the impact of the inter-electrode distance among the impellers of the anode and rings of the cathode was studied for distances between 1, 1.5 and 2 cm, as depicted in Fig. 7.

With the optimal condition (CD = 4 mA/cm^2, RT = 10 min, rotational speed = 150 rpm, pH = 4.55, and temperature = 25 °C), the most suitable efficiencies were achieved at 1 cm. During the time in which the inter-electrode distance increases from 1 to 2 cm, the removal efficiencies of the COD, TSS, and color were reduced from 97% to 95%, 97.3%–93%, and 98.30%–95%, respectively. It may be observed that with an increase in the distance among the electrodes at the same constant voltage, the electrical resistance among the electrodes increases and the collaborations among the flocs are weaker, thus causing a lower removal efficiency (Dalvand et al., 2011). With the increase in inter-electrode distance, less collaboration of the contaminants with the ionic hydroxyl is predicted; consequently, electrostatic attraction and local concentration are reduced and the removal efficiency is decreased (Abdel-Gawad et al., 2012).

3.6. Efficiency and reproducibility of the EC process performance

The main EC operation of the textile wastewater was performed at three different times to validate the performance of the application using the optimal conditions (CD = 4 mA/cm^2, RT = 10 min, rotational speed = 150 rpm, pH = 4. 57, temperature = 25 °C, and IED = 1 cm). The performance of the EC reactor was evaluated in terms of the levels of COD, TSS, color, turbidity, BOD, O & G, TDS, DO, phenols, sulfate, phosphate, nitrates and aluminum. An overall summary of the parameter results is presented in Fig. 8 and also in Table 4. The EC operation generates an overall COD removal efficiency of 97.1%. After the treatment operation, the BOD_5 and O & G within the effluent had values of 5 and 0.1 mg/L, respectively. The O & G's hydrophobic capacity leads to a superior affinity in combination with the H_2 bubbles created at the cathode. The (O & G)-H_2 complex gathers on the liquid's surface, which can be skimmed with ease (Asselin et al., 2008).

The proposed design cell of the EC allows for great efficiencies and, at the same time, reduced energy consumption, when compared to other studies. Un and Aytac (2013) investigated the treatment of textile wastewater using EC in a packed-bed electrochemical reactor. The COD removal efficiency was 96.88% and the color was almost entirely removed when the EC operated for 1 h. In contrast, in the current study, the COD removal efficiency was 97% at a reaction time of 10 min Merzouk et al. (2010) also investigated the treatment of textile wastewater using EC and electro-flotation in a batch reactor (density = 11.55 mA/cm^2, pH = 7.6, conductivity = 2.1 μS/cm and electrode gap = 1 cm). With optimal operating conditions, the following results were achieved: TSS, 85.5%; turbidity, 76.2%; BOD_5, 88.9%; COD, 79.7%; and color, 93%. When compared with the above study, the present investigation, which uses EC alone under optimal conditions, revealed great removal efficiencies: TSS, 98%; turbidity, 96%; COD, 97%; BOD_5, 95.55%; and color, over 98%. Recently, El-Ashtoukhy et al. (2013) investigated the removal of phenol from oil refinery wastewater using an electrochemical reactor with a fixed-bed anode composed of arbitrarily oriented aluminum raschig rings. At a current density of 8.59 mA/cm^2, a pH of 7, and a NaCl concentration of 1 g/L, up to 80% phenol reduction was recorded in 2 h in which the primary phenol concentration was 40 mg/L. In the current investigation, the primary phenol concentration was 350 mg/L and up to 99.99% was removed within 10 min, leaving 0.009 mg/L of phenol in the treated wastewater. Moreover, Martínez-Delgadillo et al. (2013) studied the reduction of Cr (VI) to Cr (III) by using ferrous ions [Fe (II)] in a rotating ring iron electrode. They reported a removal of 99.9% of Cr (VI) at a reaction time in the range of 42 to 22 min when the angular velocity was in the range of 0–230 rpm (at 5 A). In the present investigation, the optimal current and the reaction time were 2 A and 10 min, confirming reduced power consumption and low operational costs.

In addition, this study also demonstrated high removal of TDS (93.6%) under optimal operating conditions, and the concentration of phosphate was reduced from 7.2 to 0.23 mg/L. During the operation, the aluminum electrode dissolution exhibited an increase in the entire dissolved concentration from 1.5 to 6.00 mg/L. Compared with the global textile wastewater quality standards (EPA, 1996), the results enable the analysis of the effectiveness of the EC operation for treating the existing textile wastewater to be used for different purposes. The results revealed that the BOD, DO, TDS, turbidity and COD are all below the standard limits. However, the overall pH level of the treated wastewater was somewhat basic (6.9 ± 0.04) and is under the set limits. In a similar fashion, the grease and oil as well as the total phenols were all under the allowable limits. Using the optimal conditions, the actual consumption of electrodes was 0.038 kg/m^3, energy consumption was 4.66 kWh/m^3 where 1 kWh/m^3 for DC supply consumption and 3.66 kWh/m^3 for AC motor for rotating anode. The results showed that the main operating costs for treating one cubic meter (Eq. (1)) of wastewater at the optimum operating conditions was about 0.444 US$.

4. Conclusions

EC in textile wastewater treatment with the use of a relatively new reactor was found to have a higher efficiency when compared to previous models. The removal efficiencies of textile wastewater contaminants with relatively high values were obtained with lower current densities, specifically at 4 mA/cm^2, during the initial 10 min of reaction time at an anode rotational speed of 150 rpm and an inter-electrode distance (IED) of 1 cm. An increase in the current density improved the process performance of the EC reactor treating the textile wastewater. No requirements were found regarding fixing the pH of the solution, increasing the temperature of the solution, and adding any chemicals (NaCl or Na_2SO_4). The economical perspective of the reactor operation is affected by the operating conditions. The electrode and energy consumption of the EC increased when the current density was increased. The optimum electrodes and energy consumption were 0.038 kg/m^3 and 4.66 kWh/m^3, respectively, which resulted in lower operational costs (0.44US$/$m^3$).

Acknowledgements

The authors thank Babylon Textile Plant, Iraq for supplying the textile wastewater. They also thank Universiti Teknologi Malaysia and Ministry of Education Malaysia for funding this research under PhD scholarship fund, grant number Q.K130000.2510.10H26.

References

Abdel-Gawad, S.A., Baraka, A.M., Omran, K.A., Mokhtar, M.M., 2012. Removal of some pesticides from the simulated wastewater by electrocoagulation method using iron electrodes. Int. J. Electrochem. Sci. 7, 6654–6665.
American Public Health Association (APHA), 2000. Standard Methods for the Examination of Water and Wastewater, 20th ed. Washington, DC, USA.
Aoudj, S., Khelifa, A., Drouichea, N., Hecinia, M., Hamitouche, H., 2010. Electrocoagulation process applied to wastewater containing dyes from textile industry. J. Chem. Eng. Process. 49, 1176–1182.
Asselin, M., Drogui, P., Brar, S.K., Benmoussa, H., Blais, J.F., 2008. Organics removal in oily bilgewater by electrocoagulation process. J. Hazard. Mater. 151, 446–455.
Bayar, S., Yıldız, Y.Ş., Yılmaz, A.E., İrdemez, Ş., 2011. The effect of stirring speed and current density on removal efficiency of poultry slaughterhouse wastewater by electrocoagulation method. Desalination 280, 103–107.
Bensadok, K., Benanma, S., Lapicque, F., Nezzal, G., 2008. Electrocoagulation of cutting oil emulsions using aluminum plate electrodes. J. Hazard. Mater. 152, 423–430.
Canizares, P., Jimenez, C., Martinez, F., Rodrigo, M.A., Saez, C., 2009. The pH as a key parameter in the choice between coagulation and electrocoagulation for the treatment of wastewater. J. Hazard. Mater. 163, 158–164.
Chen, G., 2004. Electrochemical technologies in wastewater treatment. Sep. Purif. Technol. 38, 11–41.
Chen, X., Chen, G., Yue, P.L., 2000. Separation of pollutants from restaurant wastewater by electrocoagulation. Sep. Purif. Technol. 19, 65–76.
Dalvand, A., Gholami, M., Joneidi, A., Mahmoodi, N.M., 2011. Dye removal, energy consumption and operating cost of electrocoagulation of textile wastewater as a clean process. Clean – Soil Air Water 39, 665–672.
Daneshvar, N., Ashassi Sorkhabi, H., Kasiri, M.B., 2004. Decolorization of dye solution containing Acid Red 14 by electrocoagulation with a comparative investigation of different electrode connections. J. Hazard. Mater. 112, 55–62.
Daneshvar, N., Oladegaragoze, A., Djafarzadeh, N., 2006. Decolorization of basic dye solutions by electrocoagulation: an investigation of the effect of operational parameters. J. Hazard. Mater. 129, 116–122.
Drogui, P., Asselin, M., Brar, S.K., Benmoussa, H., Blais, J.F., 2008. Electrochemical removal of pollutant from agro-industry wastewater. Sep. Purif. Technol. 61, 301–310.
El-Ashtoukhy, E.-S.Z., El-Taweel, Y.A., Abdelwahab, O., Nassef, E.M., 2013. Treatment of petrochemical wastewater containing phenolic compounds by electrocoagulation using a fixed bed electrochemical reactor. Int. J. Electrochem. Sci. 8, 1534–1550.
Environmental Protection Agency (EPA), 1996. Best Management Practices for Pollution Prevention in the Textile Industry. U.S. Environmental Protection Agency, Ohio, USA. Document No. EPA/625/R-96/004.
Jaworski, Z., Dyster, K.N., Nienow, A.W., 2001. The effect of size, location and pumping direction of pitched blade turbine impellers on flow patterns: LDA measurements and CFD predictions. Trans. IChemE 79 Part A, 887–894.
Koparal, A.S., Yıldız, Y.S., Keskinler, B., Demircio_glu, N., 2008. Effect of initial pH on the removal of humic substances from wastewater by electrocoagulation. Sep. Purif. Technol. 59, 175–182.
Kresta, S.M., Wood, P.E., 1993. The flow field produced by a 45 degree pitched blade turbine: changes in the circulation pattern due to off bottom clearance. Can. J. Chem. Eng. 71, 42–53.
Laidler, K.J., Meister, J.H., 1999. Physical Chemistry, third ed. Boston.
Martínez-Delgadillo, S.A., Ramírez-Muñoz, J., Mollinedo, H.R., Mendoza-Escamilla, V., Gutiérrez- Torres, C., Jiménez-Bernal, J., 2013. Determination of the spatial distribution of the turbulent intensity and velocity field in an electrochemical reactor by CFD. Int. J. Electrochem. Sci. 8, 274–289.
Martínez-Delgadillo, S.A., Mollinedo-Ponce, H.R., Mendoza-Escamilla, V.X., Gutierrez-Torres, C., Jimenez-Bernal, J., Barrera-Diaz, C., 2012. Performance evaluation of an electrochemical reactor used to reduce Cr(VI) from aqueous media applying CFD simulations. J. Clean. Prod. 34, 120–124.
Martínez-Delgadillo, S.A., Rodríguez, M.G., Barrera-Diaz, C., 2000. A kinetic model that describes removal of chromium VI from rinsing waters of the metal finishing industry by electrochemical processes. Water Sci. Technol. 42, 55–61.
Merzouk, B., Madani, K., Sekki, A., 2010. Using electrocoagulation–electroflotation technology to treat synthetic solution and textile wastewater, two case studies. Desalination 250, 573–577.
Mishra, V.P., Dyster, K.N., Nienow, A.W., Mckemmie, J., Jaworski, Z., 1998. A study of an up- and a down-pumping wide blade hydrofoil impeller: part I. LDA measurement. Can. J. Chem. Eng. 76, 577–588.
Modirshahla, N., Behnajady, M.A., Mohammadi-Aghdam, S., 2008. Investigation of the effect of different electrodes and their connections on the removal efficiency of 4-nitrophenol from aqueous solution by electrocoagulation. J. Hazard. Mater. 154, 778–786.
Modirshahla, N., Behnajady, M.A., Kooshaiian, S., 2007. Investigation of the effect of different electrode connections on the removal efficiency of Tartrazine from aqueous solutions by electrocoagulation. Dyes Pigments 74, 249–257.
Mollah, M.Y.A., Morkovsky, P., Gomes, J.A.G., Kesmez, M., Parga, J., Cocke, D.L., 2004. Fundamentals, present and future perspectives of electrocoagulation. J. Hazard. Mater. 114, 199–210.
Nienow, A.W., 1997. On the impeller circulation and mixing effectiveness in the turbulent flow regime. Chem. Eng. Sci. 52, 2557–2565.
Oldshue, J.M., 1983. Fluid Mixing Technology. McGraw-Hill Publications Co., New York.
Paul, E.L., Atiemo-Obeng, V.A., Kresta, S.M., 2004. Handbook of Industrial Mixing Science and Practice. Wiley Interscience.
Rahim, M., Amraei, S., Alsairafi, A.A., 2011. Experimental and computational fluid dynamics modeling of mixing by visco-jet impellers. Korean J. Chem. Eng. 28, 1372–1379.
Roya, S., Acharya, S., Cloeter, M.D., 2010. Flow structure and the effect of macro-instabilities in a pitched-blade stirred tank. Chem. Eng. Sci. 65, 3009–3024.
Singh, H., Fletcher, D.F., Nijdam, J.J., 2011. An assessment of different turbulence models for predicting flow in a baffled tank stirred with a Rushton turbine. Chem. Eng. Sci. 66, 5976–5988.
Un, U.T., Aytac, E., 2013. Electrocoagulation in a packed bed reactor-complete treatment of color and cod from real textile wastewater. J. Environ. Manag. 123, 113–119.